



A seismicity burst following the 2010 M 6.4 Jiashian earthquake – implications for short-term seismic hazards in southern Taiwan

Chung-Han Chan*, Yih-Min Wu

Department of Geosciences, National Taiwan University, Taipei, Taiwan

ARTICLE INFO

Article history:

Received 12 April 2012

Received in revised form 31 July 2012

Accepted 16 August 2012

Available online 28 August 2012

Keywords:

Omori's law

Smoothing Kernel function

Coulomb stress change

Ground motion prediction equation

Probabilistic seismic hazard assessment

Taiwan

ABSTRACT

Following the 4 March 2010 M_W 6.4 Jiashian earthquake the seismicity rate in southern Taiwan was determined to be significantly higher than before the quake and aroused seismic hazard awareness. In this work, seismic hazards were investigated in terms of earthquake activity, the Coulomb stress change, the rate-and-state friction model, and short-term seismic hazard assessments. The significantly higher seismicity rate that followed the 2010 Jiashian earthquake was found to mainly be attributed to aftershock decay, in terms of the modified Omori formula. The results suggest that aftershock duration may continue until the end of 2012. The spatial migration of seismicity was modeled using the Coulomb stress changes of large earthquakes. Most of the consequent events were distributed in the vicinity of large earthquakes. The observations corresponded to a remarkable stress increase within the same area. Additionally, large events were located within regions with stress increases promoted by previous earthquakes. The results confirm interactive relationships between large events. By considering time-dependency, the seismicity rate evolution was estimated using the rate-and-state friction model. The results indicated that a high seismic rate will persist at least until the end of 2012. Short-term probabilistic seismic hazard assessments were also applied in terms of the probability of strong ground motion. Using this application, a sudden jump in seismic hazards in southern Taiwan was accompanied by each large earthquake. At the end of 2012 it is expected that hazards will return to a background level. Our results may be valuable in the future to decision-makers and public officials engaged in seismic hazard mitigation.

© 2012 Elsevier Ltd. All rights reserved.

1. Introduction

Human life and property are threatened by devastating earthquakes. For this reason, seismic hazard mitigation is an important issue for scientists and engineers. Using traditional probabilistic seismic hazard assessments (PSHAs) (McGuire, 1976; Cornell, 1968; and references therein), seismic hazards have been determined to be totally contributed by characteristic earthquakes that are independent of one another. However, for the case of the 2010 Darfield, New Zealand, earthquake sequences have determined limitations for this type of assumption (Chan et al., 2012). The Darfield sequence was initiated during the occurrence of the 4 September 2010 M 7.1 Darfield earthquake, located 40 km west of Christchurch. The earthquake caused the largest recorded peak ground acceleration (PGA), 0.3 g, in downtown Christchurch (<http://www.geonet.org.nz/earthquake/historic-earthquakes/top-nz/quake-13.html>). On 21 February 2011, the M 6.3 Christchurch earthquake took place 40 km east of the epicenter of the Darfield earthquake. In terms of spatial and temporal relationships, the

Christchurch earthquake can be regarded as an aftershock within the Darfield sequence. However, a larger PGA, of 1.88 g, was recorded in downtown Christchurch and resulted in severe damage and fatalities (<http://www.geonet.org.nz/news/feb-2011-christchurch-badly-damaged-by-magnitude-6-3-earthquake.html>). Such a circumstance points to the importance of aftershock sequences for seismic hazard evaluations. As demonstrated by the Darfield experience, a re-evaluation the seismic hazards and risks immediately following a large earthquake is required.

An increase in the seismicity rate in southern Taiwan has recently aroused awareness in seismic hazards. Since 2010, three large events with $M \geq 5.5$ have occurred – referred to as the 2010 Jiashian, the 2010 Taoyuan, and the 2012 Wutai earthquakes (the red stars in Fig. 1 and Table 1) – representing an average of 1.5 events per year. By contrast, only three large events occurred between 1900 and 2009 (the blue stars in Fig. 1), representing an average of 0.03 events per year. Some previous studies have associated the burst of seismicity with the occurrence of the 4 March 2010 M_W 6.4 Jiashian earthquake. Previous studies (Huang et al., 2011; Chen et al., submitted for publication.; Lee et al., submitted for publication.) found that an aftershock sequence followed the 2010 Jiashian earthquake, suggesting a seismicity rate increase. However, the authors did not discuss the duration of the aftershock sequence.

* Corresponding author. Tel.: +886 2 3366 4956x309; fax: +886 2 2363 6095.
E-mail address: cchan@ntu.edu.tw (C.-H. Chan).

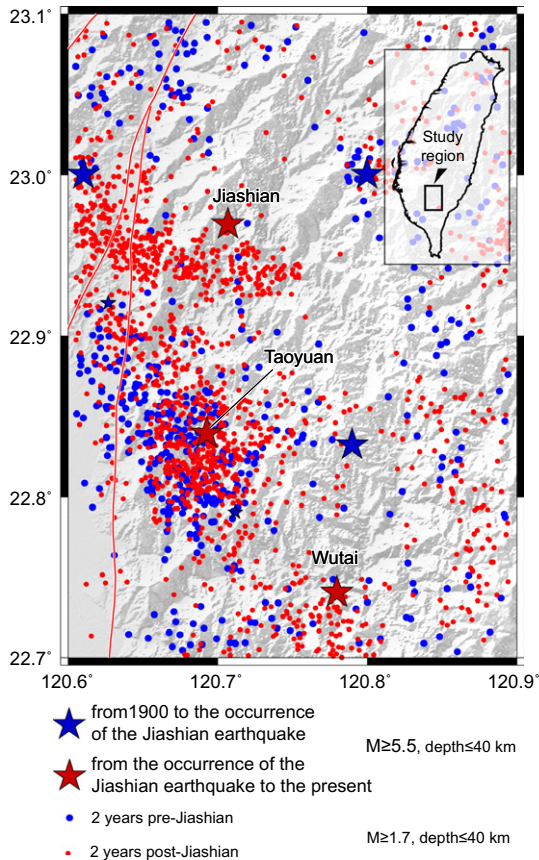


Fig. 1. Seismicity within the study region. Earthquakes with $M \geq 5.5$ and $M \geq 1.7$ are shown with stars and circles, respectively. Red lines represent the surface trace of active faults. Earthquakes shown in different colors represent various occurrence times. (For interpretation of the references to colour in this figure legend, the reader is referred to the web version of this article.)

Table 1
Rupture parameters for the source events used to calculate the seismicity rate change using the rate-and-state friction model.

Earthquake	Jiashian	Taoyuan	Wutai
Year	2010	2010	2012
Month	3	7	2
Day	4	25	26
Longitude (°)	120.70	120.74	120.78
Latitude (°)	22.96	22.84	22.74
ML	6.4	5.5	6.1
Depth (km)	23.2	16.62	20.4
Strike (°)	313	14	320
Dip (°)	41	58	20
Rake (°)	42	91	52
Fault width (km)	16.6	3.51	9.89
Fault length (km)	16.6	3.51	9.89
Avg. slip (cm)	47.86	47.86	47.86
References	Huang et al. (2011)	BATS	CWB (earthquake location) USGS/WPHASE (focal mech.)

Ching et al. (2011) and Hsu et al. (2011) modeled the Coulomb stress changes imparted by the 2010 Jiashian earthquake on active faults in southern Taiwan and estimated seismic hazards contributed by active faults. However, according to the distributions in seismicity (Fig. 1) and their corresponding focal mechanisms (Fig. 2a), the occurrence of most of the earthquakes in this region

could not be associated with the rupture of active faults (the red lines in Figs. 1 and 2). Therefore, a comprehensive study on seismic hazards in southern Taiwan is necessary.

In this study, seismic hazards in southern Taiwan are discussed in terms of earthquake activities, the Coulomb stress change, the rate-and-state friction model, and short-term seismic hazard assessments. We first discuss the spatial and temporal evolution of seismicity following the occurrence of the 2010 Jiashian earthquake. To understand the physical interpretation, the Coulomb stress changes imparted by the three large events are evaluated. To estimate earthquake evolution quantitatively, using the results of the stress evolution, the rate-and-state friction model is introduced. For evaluating seismic hazards in respect to ground motion for southern Taiwan, in this work, short-term seismic hazard assessments are also proposed.

2. The seismic activity associated with the Jiashian earthquake

2.1. The CWBSN catalog

Since 1991, the Central Weather Bureau Seismic Network (CWBSN) has been responsible for monitoring earthquake activities in Taiwan. In this network, real-time digital recording has been performed (Wu et al., 2008). Since the end of 1993, the CWBSN has turned to recording signals continuously from the trigger recording mode and has greatly enhanced earthquake monitoring capability (Wu and Chiao, 2006). To evaluate the reliability of the catalog, the magnitude of completeness (M_c), using the maximum curvature approach (Wiemer and Wyss, 2000), was calculated. A M_c of 1.7 for the study region was obtained.

2.2. The distribution of earthquakes associated with the Jiashian earthquake

As mentioned above, large earthquakes became more active following the 2010 Jiashian earthquake. In this section, the activities of smaller earthquakes are further discussed. We used the same time-interval of 2 years, before and after the 2010 Jiashian earthquake, to compare the spatial variation of earthquakes (plotted as blue and red dots, respectively, in Fig. 1). Considering the M_c of the CWBSN and crust events in this region, earthquakes with $M \geq 1.7$ and a hypocentral depth ≤ 40 km were analyzed. Similar spatial patterns were obtained for these two periods. During the post-2010 Jiashian earthquake, more earthquakes occurred in regions close to the three $M \geq 5.5$ events. In terms of the spatial distribution, consequent earthquakes following the three large events are regarded as the aftershock sequence.

In order to investigate aftershock behaviors following the 2010 Jiashian earthquake, the temporal distribution of an aftershock sequence was modeled using the modified Omori formula (Utsu, 1961), as follows:

$$n = \frac{K}{(C + t)^P}, \quad (1)$$

where n is the seismicity rate at time t since a mainshock; K is the amplitude; C is the parameter of the time offset; and P is the decay rate. In this study, K , P , and C were obtained through regression. The observed seismicity rates for each time span were tested using different time span intervals (from 1 to 30 days) and reported in the corresponding regression of the modified Omori formula. The fit of the observations between the Jiashian and Wutai earthquakes was best when a time interval of 18 days was assumed (Fig. 3a). Using this regression, the temporal distribution of consequent earthquakes following the 2010 Jiashian earthquake could be modeled as follows (Fig. 3):

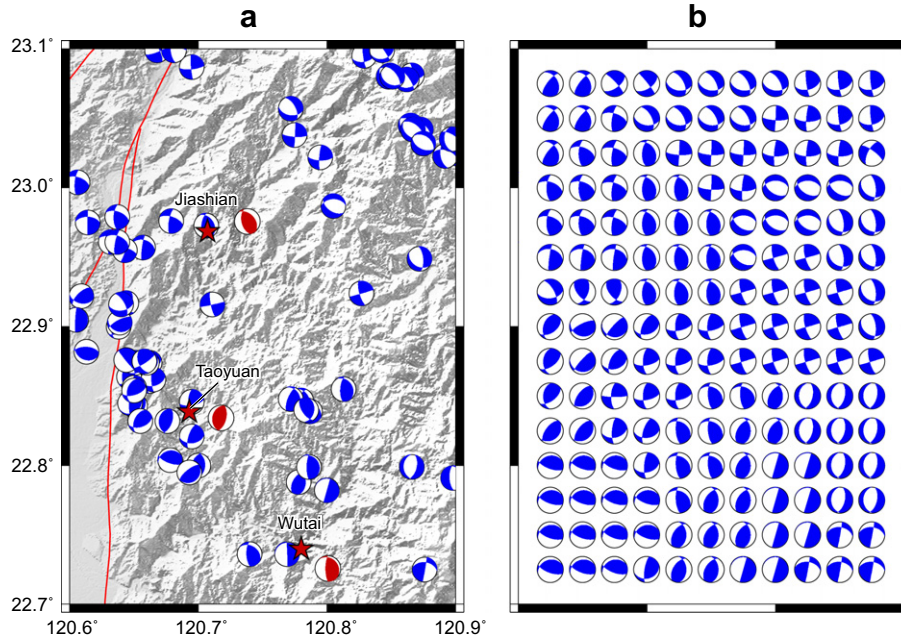


Fig. 2. (a) The reference focal mechanisms (blue) collected by Wu et al. (2010). The focal mechanisms of $M \geq 5.5$ earthquakes (red) obtained from various studies (Table 1). (b) The focal mechanisms as spatial variable receiver faults for the ΔCFS calculation. Note that the actual calculation grids ($0.01^\circ \times 0.01^\circ$) are denser than the spacing presented in the figure. (For interpretation of the references to colour in this figure legend, the reader is referred to the web version of this article.)

$$n = \frac{100.0}{(63.1 + t)^{0.74}}. \quad (2)$$

Worth mentioning here is that the relatively high C -value and low P -value could be attributed to the occurrence of the Taoyuan and Wutai earthquakes and their consequent events. According to the seismicity rate 2 years before the 2010 Jiashian earthquake, the background seismicity rate was 0.76 events per day. The seismicity rate modeled using the modified Omori formula was equal to the background seismicity rate when a t of 670 days was assumed, and can be regarded as the aftershock duration of the 2010 Jiashian earthquake. Since the time interval between the 2010 Jiashian and 2010 Taoyuan earthquakes is 143 days, the 2010 Taoyuan earthquake could be regarded as an aftershock of the 2010 Jiashian earthquake. If the standard deviation of the Omori fitting (+0.11) was considered, the aftershock duration became 970 days. The model suggests that the seismicity rate should still have been higher than background when the 2012 Wutai earthquake occurred (724 days after the 2010 Jiashian earthquake). In addition to modeling the entire sequence following the Jiashian earthquake (Fig. 3a), seismic patterns for different periods were also determined in terms of the modified Omori decay. The seismicity between the Jiashian and Taoyuan earthquakes was modeled (Fig. 3b). The modeled seismicity rate was equal to the background seismicity rate when a t of 301 days was assumed. According to this result, the 2010 Taoyuan earthquake can be regarded as an aftershock of the 2010 Jiashian earthquake. For the sequence following the Taoyuan earthquakes (Fig. 3c), a high C -value of 794 days was obtained. The pattern suggests insignificant decay during this period.

Since the estimated aftershock durations were long for such moderately-sized earthquakes, seismicity following the 2010 Jiashian and Taoyuan earthquakes could not solely be explained as an aftershock pattern. To determine aftershock behaviors for different aspects, a time series of the seismicity rate within the study region was determined (Fig. 4). Following the occurrence of each large event the time series displayed a sudden increase in the seismicity rate. However, the seismicity rate remained at a high level for sev-

eral months following the 2010 Taoyuan earthquake (Fig. 4). The seismicity rate between 3 months following the 2010 Taoyuan and 2012 Wutai earthquakes was 43% higher than background. Such a continuously high rate level could not be modeled using the modified Omori formula (as shown in Eq. (2)).

The earthquake distribution during different periods represents the many events that have occurred in the vicinity of previously occurring larger events (Fig. 5). The observations could be associated with aftershock decays. Worth mentioning here is that some of the earthquakes took place in the vicinity of the 2010 Taoyuan earthquake before the occurrence of this earthquake (light gray dots in Fig. 5). Such an observation may imply an interaction between the 2010 Jiashian earthquake and the fault system near Taoyuan.

Through the spatial-temporal distribution of earthquakes within the study region, some patterns of earthquake activity could not simply be explained by aftershock behavior using the modified Omori formula. In the discussion that follows, the Coulomb stress change and the rate-and-state friction model are introduced in order to model the observation.

3. The Coulomb stress changes imparted by the three large earthquakes

3.1. The procedure and the parameter setting

The general expression of the ΔCFS (Coulomb stress change) can be represented as follows (Harris, 1998; Cocco and Rice, 2002):

$$\Delta CFS = \Delta \tau + \mu' \Delta \sigma_n, \quad (3)$$

where $\Delta \tau$ is the shear stress change computed along the slip direction on the receiver fault; μ' is the apparent friction coefficient; and $\Delta \sigma_n$ is the normal stress change perpendicular to the receiver fault.

The focal mechanism responsible for the receiver fault is a key parameter for ΔCFS calculations. Generally, it can be represented in the following forms: (1) optimally oriented fault planes through a combination of the regional stress field and a stress change

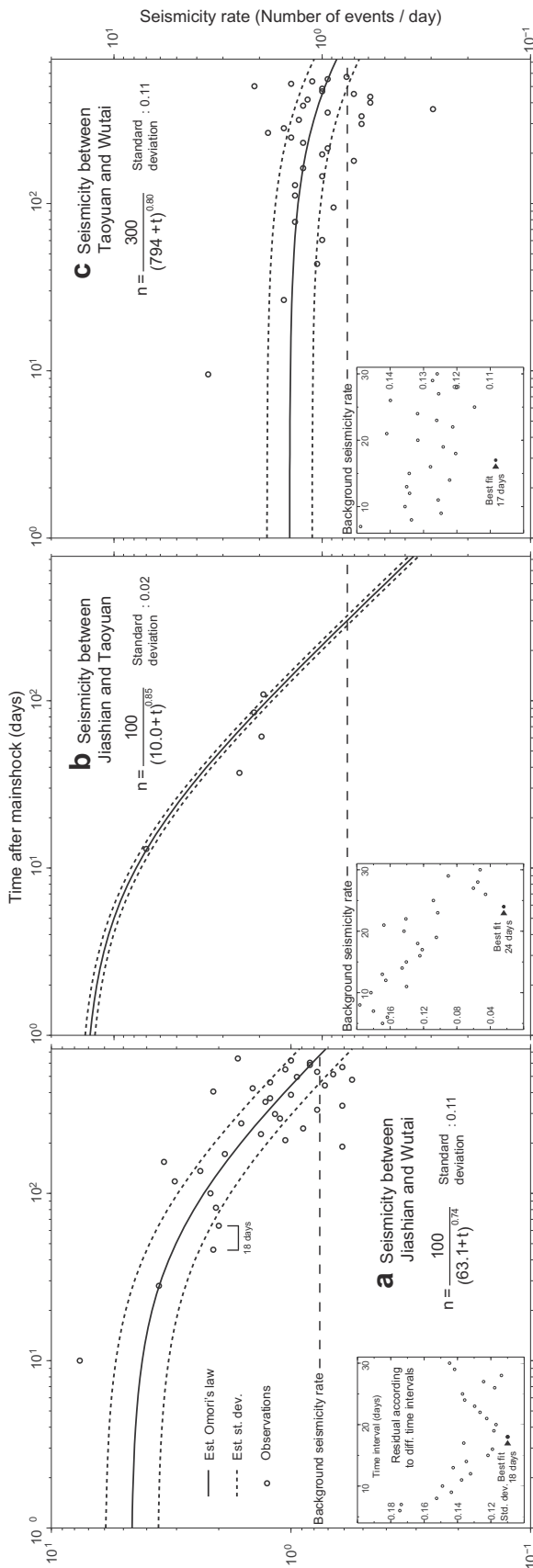


Fig. 3. Observations and the modeled temporal earthquake distribution following the 2010 Jiashian mainshock. The modeled distribution was obtained using the modified Omori formula. The residuals between the various observations and the models obtained using different time intervals are shown in the inset.

caused by the source event (King et al., 1994); (2) mechanisms of active faults (Toda et al., 1998); and (3) different focal mechanisms of earthquakes in sub-regions (Chan and Stein, 2009). For the study region, since the stress field in terms of the orientation and the magnitude remains controversial, it is difficult to apply optimally oriented fault planes as receiver faults. Additionally, most of the earthquakes occurring in this study region are rarely related to the rupture of active faults (Figs. 1 and 2a). Therefore, it is not practical to assume that active faults are receivers. Using this information we followed the procedure outlined in previous studies (Chan et al., 2010; Hainzl et al., 2010; Toda and Enescu, 2011) and assumed spatially variable receiver faults for each calculation grid. The focal mechanisms determined by Wu et al. (2010) were introduced as a reference (Fig. 2a). The spatial variable receiver fault was assumed to consist of the reference focal mechanism with the shortest epicentral distance to each specified grid (Fig. 2b). The ΔCFS on each $0.01^\circ \times 0.01^\circ$ grid was estimated using a spatial variable receiver fault by applying the COULOMB 3.2 program (Toda and Stein, 2002). We followed the procedures proposed by Catalli and Chan (2012) and reported the maximum ΔCFS among seismogenic depths for each calculation grid. Using these procedures, the uncertainties of earthquake location and the rupture geometry for the calculation could be minimized.

3.2. The slip models of the three events

An application of Coulomb model calculations requires knowledge of the rupture parameters for source events, such as the geometry of the rupturing fault and the slip magnitude. In Taiwan, these relationships were scaled by Yen and Ma (2011) as follows:

$$\text{Log}(L) = (1/2)\text{log}M_0 - 8.08; \quad (4)$$

$$\text{Log}(W) = (1/2)\text{log}M_0 - 8.08; \quad (5)$$

$$\text{Log}(AD) = 1.68; \quad (6)$$

where L is the fault length in kilometers; M_0 is the seismic moment in Newton-meter; W is the fault width in kilometers; and AD is the average slip in centimeters. In order to evaluate the seismic moment using the local magnitude, M_w , and the local magnitude, M_L , should be introduced. We used the relationship by Wu et al. (2005), who considered earthquakes with $4.7 \geq M_w \geq 6.2$ in Taiwan, as follows:

$$M_w = M_L - 0.2. \quad (7)$$

According to the relationship and the source parameters of each earthquake, the rupture parameters were assumed to be those listed in Table 1.

3.3. The correlation of the distribution with consequence events

The ΔCFS imparted by the 2010 Jiashian, the 2010 Taoyuan, and the 2012 Wutai earthquakes was evaluated (Fig. 6). The results indicated a remarkable increase in ΔCFS in the vicinity of each event, and decay with the epicentral distance. Additionally, the 2010 M 6.4 Jiashian earthquake (Fig. 6a) caused a wider and larger stress increase. By contrast, the 2010 M 5.5 Taoyuan earthquake caused less significant stress changes. Such a discrepancy can be attributed to the magnitude difference between the two events (Table 1). Additionally, it appears that the distribution of the ΔCFS of earthquakes can be associated with the distribution of consequent events. Following the occurrence of each event (Fig. 6), most of the consequent events were distributed in its vicinity. The greater number of earthquakes following the 2010 Jiashian mainshock could be associated with the corresponding ΔCFS pattern (Fig. 6a).

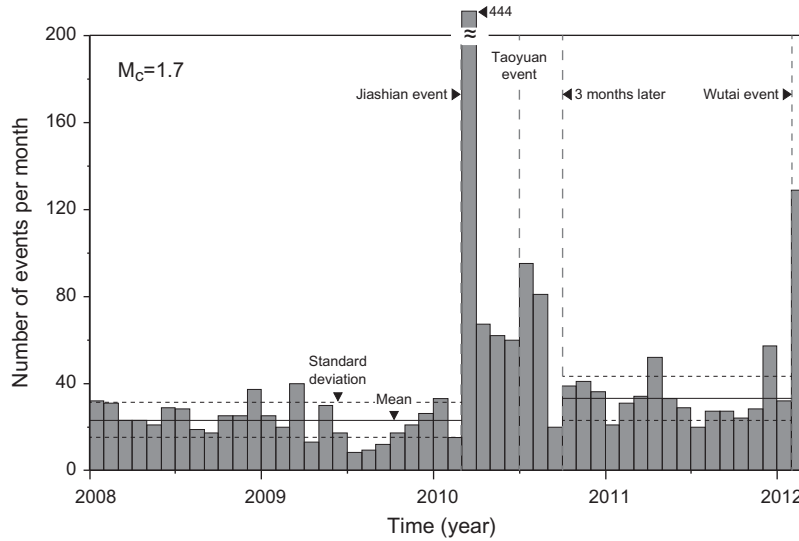


Fig. 4. The time series of earthquakes within the study region since 2008; $M \geq 1.7$ earthquakes were considered. The mean values and the standard deviations of the seismicity rates for various periods are represented by solid and dashed lines, respectively.

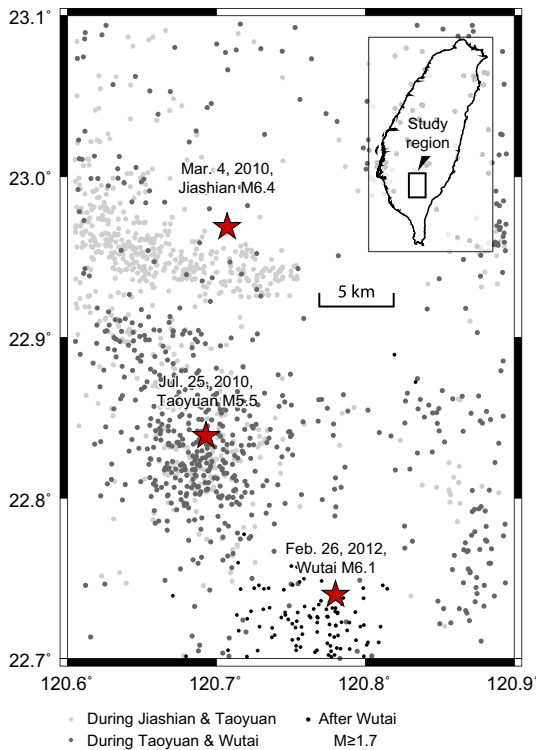


Fig. 5. The seismicity of different periods within the study region; earthquakes larger than 1.7 were considered. Earthquakes shown with different colors represent different occurrence times. Red lines represent the surface trace of active faults. (For interpretation of the references to colour in this figure legend, the reader is referred to the web version of this article.)

3.4. The interactions between large events

A correlation between the ΔCFS and the occurrence of small events was obtained. However, in respect to seismic hazards, larger earthquakes were more important. In respect to determining seismic hazards, the stress change for each consequent event was evaluated (Fig. 6). As imparted by the 2010 Jiashian earthquake, the stress changes determined for the 2010 Taoyuan and

2012 Wutai epicenters were +1.78 and +0.20 bars, respectively. The results suggest that the 2010 Jiashian earthquake promoted failure on fault systems near the epicenters of the 2010 Taoyuan and the 2012 Wutai earthquakes. As imparted by the 2010 Taoyuan earthquake, the stress change determined for the epicenter of the 2012 Wutai earthquake was +0.03 bars, a value higher than the magnitude of tidal triggering (+0.01 bars) as observed by Stein (2004).

4. The seismic rate evolution modeled using the rate-and-state friction model

4.1. The procedure and parameter setting

Above, the ΔCFS of the earthquakes are presented. In order to quantify the impact of the ΔCFS on the seismicity rate, the rate-and-state friction model (Dieterich, 1994) was used. We followed Chan et al. (2010) and determined the evolution of the seismicity rate $R(M, x, t)$ using the ΔCFS of the n th source event $\Delta CFS_n(x)$ at the site of interest, x , as a function of the magnitude, M , and the time, t , as follows:

$$R(M, x, t) = \frac{\lambda(M, x)}{\left[\frac{\lambda(M, x)}{R_{n-1}(M, x)} \exp\left(-\frac{\Delta CFS_n(x)}{A\sigma}\right) - 1 \right] \exp\left(-\frac{t-t_n}{t_{na}}\right) + 1}, \quad (8)$$

where $R_{n-1}(M, x)$ is the short-term seismicity rate promptly before the occurrence of the n th source event (i.e. $R_0 = \lambda(M, x)$); $A\sigma$ is a constitutive parameter of the model as described by Dieterich (1994); t_n is the occurrence time of the n th source event; and t_{na} is the aftershock duration. The relationship describes the short-term seismicity rate evolution by considering a series of source events and presents a generalization of the relationships.

Previous studies (e.g. Catalli et al., 2008; Nakata et al., 2008) have proposed several analysis approaches for obtaining the value of $A\sigma$. However, the acquirement of this parameter for the study region is beyond the scope of this work. In order to reduce the number of assumptions in the model, a fixed value of 0.4 bars for $A\sigma$ was assumed. The value is in accordance with physically reasonable ranges between 0.1 and 0.4 bars (Catalli et al., 2008; Chan et al., 2012; Toda and Stein, 2003; Toda et al., 2005). A t_{na} of 670 days was assumed, corresponding to the aftershock duration of the 2010 Jiashian mainshock (Fig. 3).

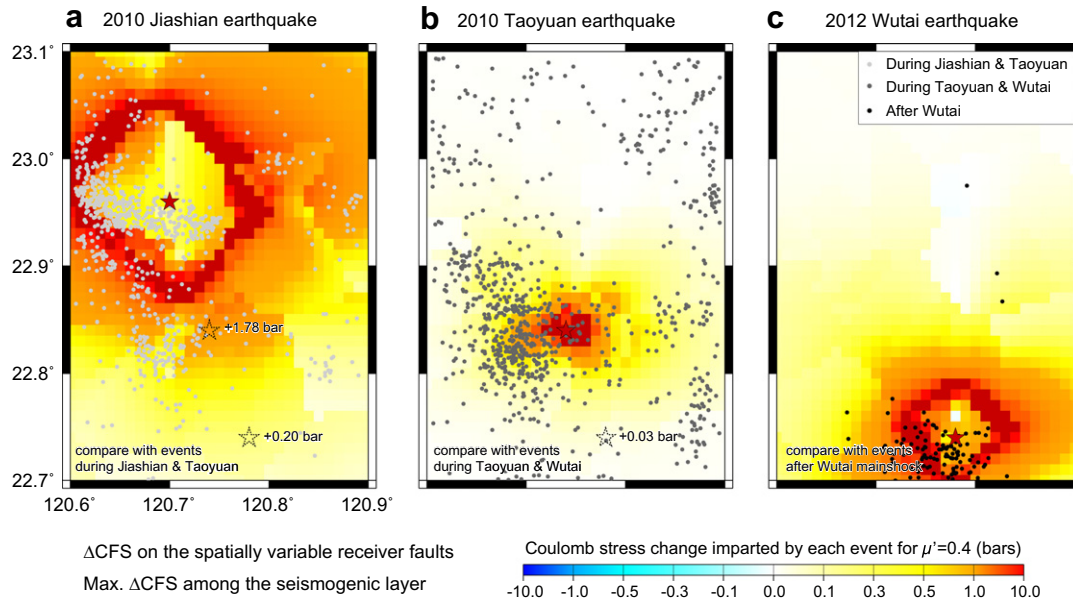


Fig. 6. The Coulomb stress change imparted by the (a) 2010 Jiashian, (b) 2010 Taoyuan, and (c) 2012 Wutai earthquakes. The stress changes solved for each large earthquake (denoted as dashed stars) are represented.

4.2. Results

A seismicity rate evolution for southern Taiwan was calculated using the rate-and-state friction model (Fig. 7). Remarkable increases were determined for the seismicity rate within the region close to the three $M \geq 5.5$ earthquakes. By contrast, in regions far from earthquakes, rate perturbations were insignificant. Rate

decay with time is illustrated here with rate changes at various time spots (e.g. Fig. 7a and b). Note that the results suggest that the seismicity rate near the 2012 Wutai epicenter should remain high until the end of 2012 (Fig. 7f). To associate the calculated rates with the occurrence of large events, we found an increase in seismicity rate by 396% at the epicenter of the 2010 Taoyuan earthquake, immediately prior to its occurrence (Fig. 7b). Additionally,

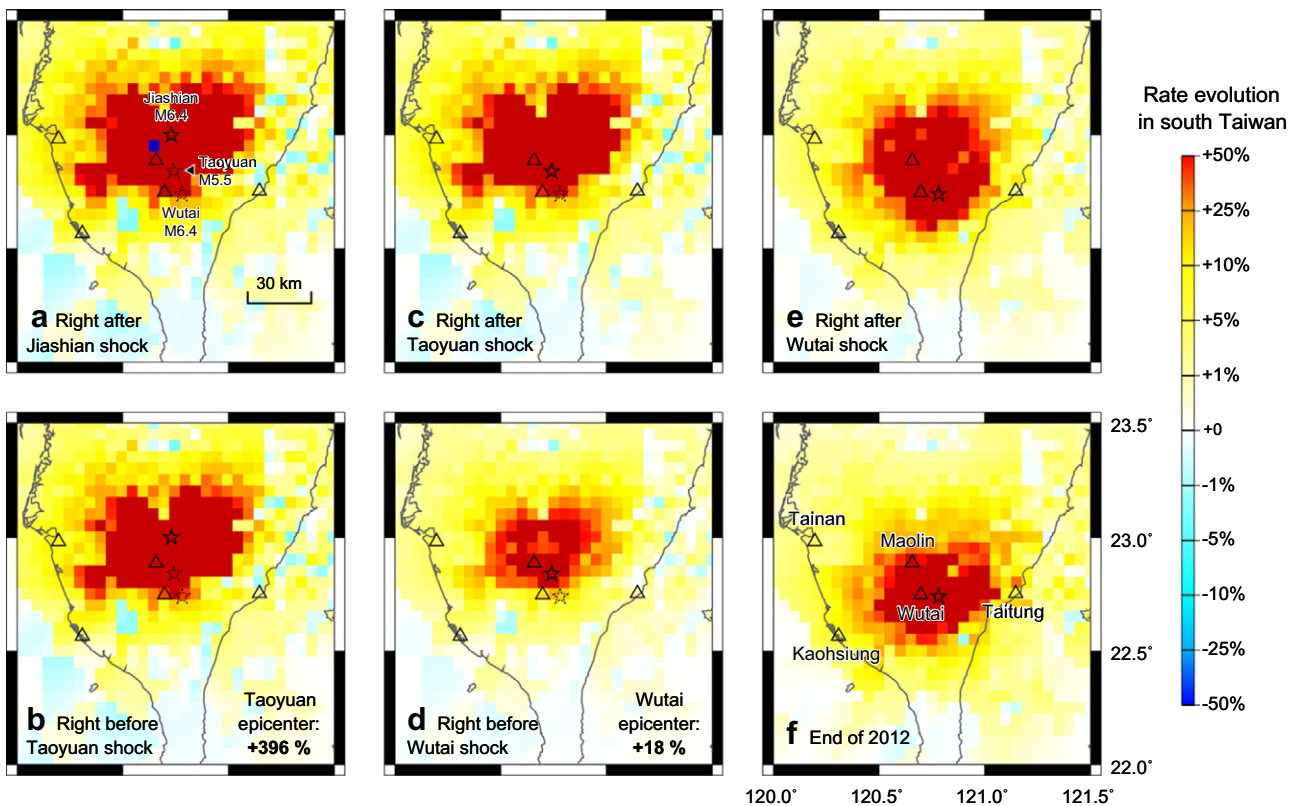


Fig. 7. The modeled short-term seismicity rate change determined using the rate-and-state friction model at various locations. Rupture parameters for the three source events of the rate change calculations are shown in Table 1. The rate change before the Taoyuan and Wutai earthquakes is shown in (b) and (d), respectively. Triangles represent the five cities used for short-term seismic hazard evaluations (Fig. 8).

a slight increase in the seismicity rate by 18% was obtained at the epicenter of the 2012 Wutai earthquake (Fig. 7d).

5. Discussion

5.1. Earthquake interactions since the Jiashian earthquake

Several models have been proposed for the relationships between the earthquakes in southern Taiwan that have occurred since 2010. Temporal aftershock behavior following the 2010 Jiashian mainshock was forecast using the modified Omori formula (Fig. 3). The results indicate that the 2010 Taoyuan and 2012 Wutai earthquakes could be regarded as aftershocks of the 2010 Jiashian mainshock. Additionally, the result also suggests a higher seismic hazard due to the 2010 Jiashian earthquake sequence until the end of 2012. In order to model the stress evolution, the ΔCFS imparted by the three earthquakes was calculated (Fig. 6). A remarkable ΔCFS increase was obtained in the vicinity region of each epicenter, where most consequent earthquakes take place (Fig. 6). The results also confirmed interactive relationships between these three large events. By further considering the time-dependency, the seismicity rate evolution in southern Taiwan was evaluated using the rate-and state friction model (Fig. 7). In addition to the similar spatial pattern of the ΔCFS (Fig. 6), the temporal rate evolution is illustrated and shows a decay in the seismicity rate following a larger event. The result corresponds to a pattern of aftershock decay (Fig. 3). Moreover, the modeled seismicity rate remained continuously high following the 2010 Jiashian earthquake, possibly associated with a significantly higher rate following the 2010 Jiashian earthquake (Fig. 4). According to the ΔCFS model a higher seismicity rate is expected as a result of the occurrence of the 2010 Jiashian earthquake. Considering the rate-and-state friction model, high seismic hazards could persist at least until the end of 2012. A higher rate is expected if another large event occurs.

5.2. The evolution of seismic hazards in terms of the short-term PSHA

The short-term PSHAs (probabilistic seismic hazard assessments), in terms of the probability of strong ground motion, were evaluated for some of the cities in southern Taiwan. We followed the approach proposed by Chan et al. (2012) and Chan et al. (submitted for publication). Using this approach, the background seismicity rate was obtained through the zoneless approach of Woo

(1996). The approach was summed over all of the events in the complete catalog and divided by the corresponding duration. To build up the background rate model, earthquakes with $M \geq 5.0$, since 1940 were, considered since all earthquakes that pass this threshold in magnitude and time are recorded by the CWBSN (Chan et al., submitted for publication). Then, the short-term rate perturbation was evaluated using the rate-and-state friction model (Eq. (8)). In addition to a reliable seismicity rate model, another item that should be considered for a PSHA is ground motion behaviors due to path and site effects. For path effects, ground motion prediction equations (GMPEs) were introduced. Since several studies (Crouse et al., 1988 and references therein) have pointed out that the attenuation behaviors for subduction earthquakes and crustal earthquakes are different, the GMPEs obtained by Lin (2009) and Lin and Lee (2008) were considered for crustal and subduction events, respectively. To consider site amplification, we introduced the averaged shear-velocity down to 30 m (V_s30) at the CWBSN and Taiwan Strong Motion Instrumentation Program (TSMIP) stations as obtained by Lee and Tsai (2008). Information from these five stations, CHY125, KAU069, KAU077, TTN, and KAU, was used to present site amplifications for the cities of Tainan, Maolin, Wutai, Taitung, and Kaohsiung, respectively.

Through the procedure and parameters mentioned above, the short-term PSHA was applied to the five cities in southern Taiwan (Fig. 8). Prior to the 2010 Jiashian earthquake, the seismic hazard in Taitung was the highest amongst the five cities. The lowest hazard was determined for the city of Kaohsiung. The results correspond to previous results (Cheng, 2002; Cheng et al., 2007; Campbell et al., 2002) where traditional PSHA approaches were applied (Cornell, 1968; McGuire, 1976). Following the Jiashian earthquake, a sudden jump in seismic hazards was determined for all of the cities. The highest hazard was found for Maolin, since it has the shortest epicentral distance to the 2010 Jiashian earthquake. Other abrupt seismic hazard increases were accompanied by the 2010 Taoyuan and 2012 Wutai earthquakes. The hazards level occurring at the end of 2012 is expected to be similar to background.

5.3. Seismic hazard maps following the occurrence of the three earthquakes

The evolution of seismic hazards in some of the cities in southern Taiwan during 2010 and 2013 are presented in Fig. 8. The results indicate that significantly higher hazards followed the three

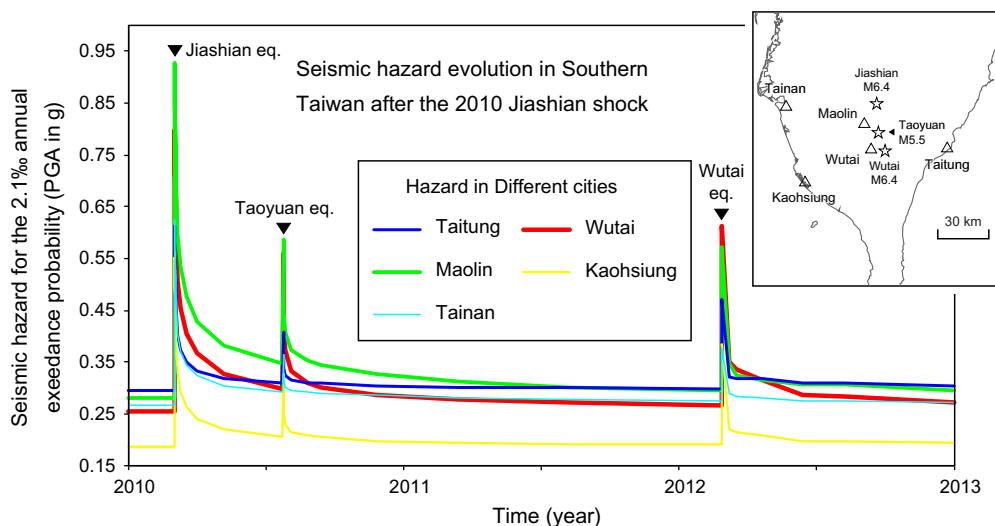


Fig. 8. The temporal evolution of seismic hazards for the 2.1% annual exceedance probability in five cities (triangles in the inset). Variations in seismic hazards are attributed to the seismicity rate change imparted by large events (Fig. 7).

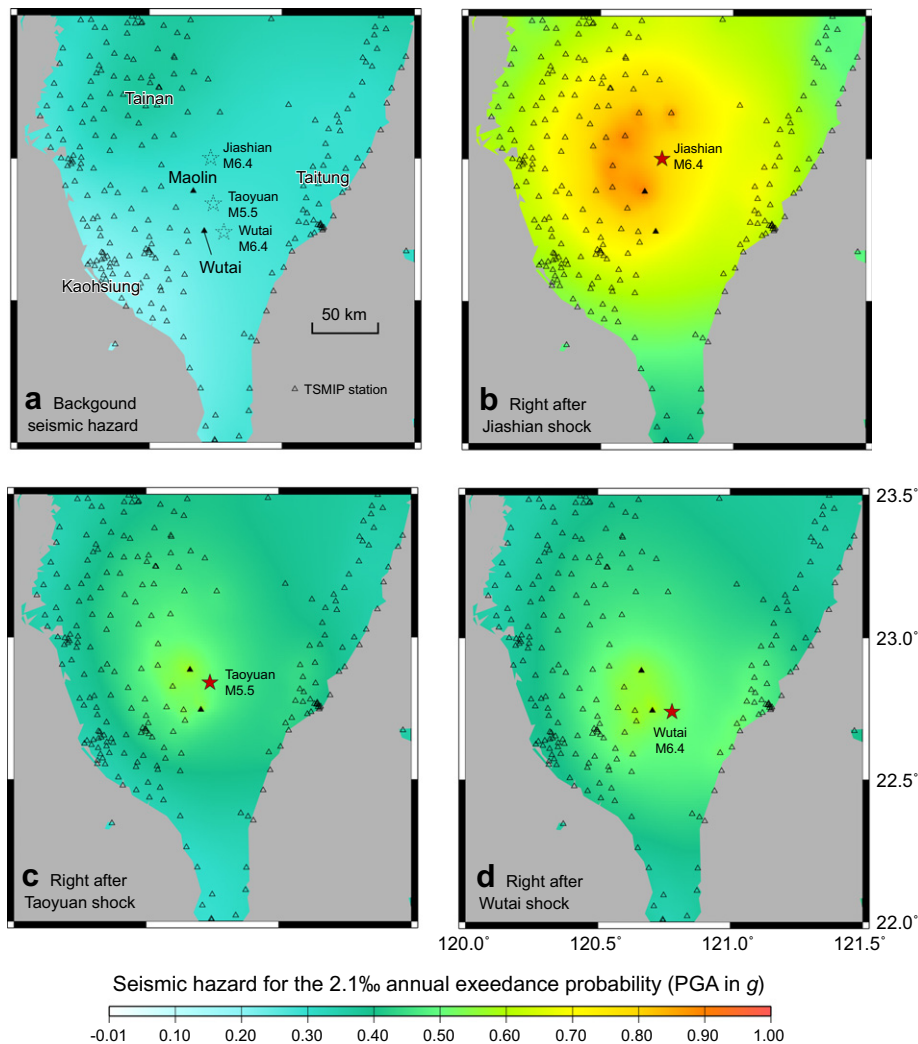


Fig. 9. The seismic hazard maps, as follows: (a) before Jiashian, (b) immediately following Jiashian, (c) immediately following Taoyuan, and (d) immediately following Wutai. Stars represent the epicenters of the three earthquakes. Triangles represent the TSMIP and CWBSN stations.

$M \geq 5.5$ earthquakes. Here, the spatial distribution of seismic hazards is further evaluated. Site amplification for each site (triangles in Fig. 9) was considered using a function of $V_s/30$ as obtained by Lee and Tsai (2008). Seismic hazard maps at various time spots were evaluated. Before the perturbations (Fig. 9a), higher hazards were determined in the Tainan and Taitung regions; within the Kaohsiung region, in contrast, the hazard was relatively low. Such a result corresponds to the temporal evolution of seismic hazards prior to the 2010 Jiashian earthquake (Fig. 8). Following the occurrence of the Jiashian earthquake (Fig. 9b), significantly higher hazards were determined at the periphery of the epicenter. Note that the higher hazard in the west can be attributed to shorter epicentral distances for stations in this direction. Following the occurrence of the Taoyuan and Wutai earthquakes (Fig. 9c and d), the seismic hazard peaks migrated to the south, corresponding to the migration of seismicity activities (Fig. 5). Such results could provide essential information for emergency response regarding victim sheltering and relocation immediately following a devastating earthquake.

6. Conclusions

With various aspects (i.e. earthquake activities, the Coulomb stress change, the rate-and-state friction model, and short-term

seismic hazard assessments), here, seismic hazards for southern Taiwan have been outlined. All of the results suggest a larger amount of hazards following the 2010 Jiashian earthquake. The increase in hazards could be sustained for several months following the 2012 Wutai earthquake (as suggested by the results of the short-term seismic hazard assessment) or longer (as suggested by the results of the ΔCFS and the rate-and-state friction model). Our results may be valuable in the future to decision-makers, public officials, and engineers engaged in seismic hazard mitigation. One possible application of our results is to provide probabilistic seismic hazard information following the occurrence of a devastating earthquake. The probability of time dependent ground motion levels can be assessed using our approach. Such results could provide important information for emergency response regarding victim sheltering and relocation. Another possible application is a combination with deterministic earthquake scenarios. Scenarios are also useful for proposals of seismic hazard mitigation, in terms of building codes and the site selection of public structures (McGuire, 2001). The occurrence probability of a scenario earthquake can be re-evaluated following a neighboring large earthquake. Such estimations could be performed using the de-aggregation and determination of dominant earthquakes. Additionally, our approach provides different insights for seismic hazards, and can be considered as a branch of the logic-tree approach for PSHA.

Acknowledgements

Our work was supported by the National Science Council and the Central Weather Bureau in Taiwan. We thank Prof. Bor-ming Jahn and three anonymous reviewers for their constructive comments.

References

- Campbell, K.W., Thenhaus, P.C., Barnard, T.P., Hampson, D.B., 2002. Seismic hazard model for loss estimation and risk management in Taiwan. *Soil Dynamics and Earthquake Engineering* 22, 743–754. [http://dx.doi.org/10.1016/S0267-7261\(02\)00095-7](http://dx.doi.org/10.1016/S0267-7261(02)00095-7).
- Catalii, F., Chan, C.H., 2012. New insights into the application of the Coulomb model in real time. *Geophysical Journal International* 188, 583–599. <http://dx.doi.org/10.1111/j.1365-246X.2011.05276.x>.
- Catalii, F., Cocco, M., Console, R., Chiaraluca, L., 2008. Modeling seismicity rate changes during the 1997 Umbria-Marche sequence (central Italy) through a rate- and state-dependent model. *Journal of Geophysical Research* 113, B11301. <http://dx.doi.org/10.1029/2007JB005356>.
- Chan, C.H., Stein, R.S., 2009. Stress evolution following the 1999 Chi-Chi, Taiwan, earthquake: consequences for afterslip, relaxation, aftershocks, and departures from Omori decay. *Geophysical Journal International*. doi: 10.1111/j.1365-246X.2008.04069.x.
- Chan, C.H., Sørensen, M.B., Stromeyer, D., Grünthal, G., Heidebach, O., Hakimhashemi, A., Catalii, F., 2010. Forecasting Italian seismicity through a spatio-temporal physical model: importance of considering time dependency and reliability of the forecast. *Annals of Geophysics* 53 (3). <http://dx.doi.org/10.4401/ag-4761>.
- Chan, C.H., Wu, Y.M., Lin, T.L., 2012. A short term seismic hazard assessment in Christchurch, New Zealand, after the M 7.1, 4 September 2010 Darfield earthquake: an application of a smoothing Kernel and rate-and-state friction model. *Terrestrial Atmospheric and Oceanic Sciences* 23 (2), 1. [http://dx.doi.org/10.3319/TAO.2011.09.23.02\(T\)](http://dx.doi.org/10.3319/TAO.2011.09.23.02(T)).
- Chan, C.H., Wu, Y.M., Cheng, C.T., Lin, P.S., submitted for publication. Short-term probabilistic seismic hazard assessment and its application to Hualien City, Taiwan.
- Chen, C.H., Wen, S., Yeh, T.K.; Wang, C.H., Yen, H.Y., Liu, J.Y., Hobara, Y., submitted for publication. The tectonic implication of the Jiashian earthquake ($M=6.4$) in Taiwan.
- Cheng, C.T., 2002. Uncertainty analysis and de-aggregation of seismic hazard in Taiwan. PhD Dissertation. Institute of Geophysics, National Central University, Chung-Li, Taiwan (in Chinese).
- Cheng, C.T., Chiou, S.J., Lee, C.T., Tsai, Y.B., 2007. Study on probabilistic seismic hazard maps of Taiwan after Chi-Chi earthquake. *Journal of GeoEngineering* 2 (1), 19–28.
- Ching, K.E., Johnson, K.M., Rau, R.J., Chuang, R.Y., Kuo, L.C., Leu, P.L., 2011. Inferred fault geometry and slip distribution of the 2010 Jiashian, Taiwan, earthquake is consistent with a thick-skinned deformation model. *Earth and Planetary Science Letters*, EPLS-S-10-00445. doi: 10.1016/j.epsl.2010.10.021.
- Cocco, M., Rice, J.R., 2002. Pore pressure and poroelasticity effects in Coulomb stress analysis of earthquake interactions. *Journal of Geophysical Research* 107 (B2), 2030. <http://dx.doi.org/10.1029/2000JB000138>.
- Cornell, C.A., 1968. Engineering seismic risk analysis. *Bulletin of the Seismological Society of America* 58, 1583–1606.
- Crouse, C.B., Vyas, Y.K., Schell, B.A., 1988. Ground motion from subduction-zone earthquakes. *Bulletin of the Seismological Society of America* 78 (1), 1–25.
- Dieterich, J.H., 1994. A constitutive law for rate of earthquake production and its application to earthquake clustering. *Journal of Geophysical Research* 99 (18), 2601–2618.
- Hainzl, S., Zoeller, G., Wang, R., 2010. Impact of the receiver fault distribution on aftershock activity. *Journal of Geophysical Research* 115, B05315. <http://dx.doi.org/10.1029/2008JB006224>.
- Harris, R.A., 1998. Introduction to special section: stress triggers, stress shadows, and implications for seismic hazard. *Journal of Geophysical Research* 103, 24347–24358.
- Hsu, Y.R., Yu, S.B., Kuo, L.C., Tsai, Y.C., Chen, H.Y., 2011. Coseismic deformation of the 2010 Jiashian, Taiwan earthquake and implications for fault activities in southwestern Taiwan. *Tectonophysics* 502, 328–335.
- Huang, H.H., Wu, Y.M., Lin, T.L., Chao, W.A., Shyu, J.B.H., Chan, C.H., Chang, C.H., 2011. The Preliminary Study of the 4 March 2010 M_w 6.3 Jiashian, Taiwan. Earthquake Sequence, *Terrestrial Atmospheric and Oceanic Sciences* 22 (3), 283–290. [http://dx.doi.org/10.3319/TAO.2010.12.13.01\(T\)](http://dx.doi.org/10.3319/TAO.2010.12.13.01(T)).
- King, G.C.P., Stein, R.S., Lin, J., 1994. Static stress changes and the triggering of earthquakes. *Bulletin of the Seismological Society of America* 84, 935–953.
- Lee, C.T., Tsai, B.R., 2008. Mapping V_s30 in Taiwan. *Terrestrial Atmospheric and Oceanic Sciences* 19 (6). [http://dx.doi.org/10.3319/TAO.2008.19.6.671\(PT\)](http://dx.doi.org/10.3319/TAO.2008.19.6.671(PT)).
- Lee, S.J., Mozziconacci, L., Liang, W.T., Hsu, Y.J., Lu, C.Y., Huang, W.G., Huang, B.S., submitted for publication. Source complexity of the 4 March 2010 Jiashian, Taiwan, Earthquake determined by joint inversion of teleseismic and near field data.
- Lin, P.S., 2009. Ground-motion attenuation relationship and path-effect study using Taiwan Data set. Ph.D. Dissertation. Institute of Geophysics, National Central University, Chung-Li, Taiwan (in Chinese).
- Lin, P.S., Lee, C.T., 2008. Ground-motion attenuation relationships for subduction-zone earthquakes in northeastern Taiwan. *Bulletin of the Seismological Society of America* 98 (1), 220–240. <http://dx.doi.org/10.1785/0120060002>.
- McGuire, R., 1976. FORTRAN computer program for seismic risk analysis. US Geological Survey, Open-File Rept. 76–67, 90 pp.
- McGuire, R., 2001. Deterministic vs. probabilistic earthquake hazard and risks. *Soil Dynamics and Earthquake Engineering* 21, 377–384.
- Nakata, R., Suda, N., Tsuruoka, H., 2008. Non-volcanic tremor resulting from the combined effect of Earth tides and slow slip events. *Nature Geoscience* 1, 676–678.
- Stein, R.S., 2004. Tidal triggering caught in the act. *Science* 305, 1248–1249.
- Toda, S., Enescu, B., 2011. Rate/state Coulomb stress transfer model for the CSEP Japan seismicity forecast. *Earth, Planets and Space* 63, 171–185. <http://dx.doi.org/10.5047/eps.2011.01.004>.
- Toda, S., Stein, R.S., 2002. Response of the San Andreas fault to the 1983 Coalinga-Nuñez earthquakes: an application of interaction-based probabilities for Parkfield. *Journal of Geophysical Research* 107. <http://dx.doi.org/10.1029/2001JB000172>.
- Toda, S., Stein, R.S., 2003. Toggling of seismicity by the 1997 Kagoshima earthquake couplet: a demonstration of time-dependent stress transfer. *Journal of Geophysical Research* 108 (B12), 2567. <http://dx.doi.org/10.1029/2003JB002527>.
- Toda, S., Stein, R.S., Reasenberg, P.A., Dieterich, J.H., Yoshida, A., 1998. Stress transferred by the $M_w = 6.9$ Kobe, Japan, shock: effect on aftershocks and future earthquake probabilities. *Journal of Geophysical Research* 103, 24543–24565.
- Toda, S., Stein, R.S., Richards-Dinger, K., Bozkurt, S.B., 2005. Forecasting the evolution of seismicity in southern California: animations built on earthquake stress transfer. *Journal of Geophysical Research* 110 (B5), B05S16.
- Utsu, T., 1961. Statistical study on the occurrence of aftershocks. *Geophysical Magazine* 30, 521–605.
- Wiemer, S., Wyss, M., 2000. Minimum magnitude of completeness in earthquake catalogs: examples from Alaska, the Western United States, and Japan. *Bulletin of the Seismological Society of America* 90 (4), 859–869.
- Woo, G., 1996. Kernel estimation methods for seismic hazard area source modeling. *Bulletin of the Seismological Society of America* 86, 353–362.
- Wu, Y.M., Chiao, L.Y., 2006. Seismic quiescence before the 1999 Chi-Chi, Taiwan M_w 7.6 earthquake. *Bulletin of the Seismological Society of America* 96, 321–327.
- Wu, Y.M., Allen, R.M., Wu, C.F., 2005. Revised M_i determination for crustal earthquakes in Taiwan. *Bulletin of the Seismological Society of America* 95, 2517–2524.
- Wu, Y.M., Chang, C.H., Zhao, L., Teng, T.L., Nakamura, M., 2008. A comprehensive relocation of earthquakes in Taiwan from 1991 to 2005. *Bulletin of the Seismological Society of America* 98, 1471–1481. <http://dx.doi.org/10.1785/0120070166>.
- Wu, Y.M., Hsu, Y.J., Chang, C.H., Teng, L.S., Nakamura, M., 2010. Temporal and spatial variation of stress field in Taiwan from 1991 to 2007: insights from comprehensive first motion focal mechanism catalog. *Earth and Planetary Science Letters* 298, 306–316. <http://dx.doi.org/10.1016/j.epsl.2010.07.047>.
- Yen, Y.T., Ma, K.F., 2011. Source-scaling relationship for M 4.6–8.9 earthquakes, specifically for earthquakes in the collision zone of Taiwan. *Bulletin of the Seismological Society of America* 101 (2). <http://dx.doi.org/10.1785/0120100046>.